The Effect of MR Acoustic Noise on FDG-PET Uptake in a Simultaneous MR/PET System

D. B. Chonde[1,2], N. Abolmaali[3], A. G. Sorensen[1], and C. Catana[1]
[1]Athinoula A. Martinos Center for Biomedical Imaging, Charlestown, MA, United States, [2]Department of Biophysics, Harvard University, Cambridge, MA, [3]OncoRay - Center for Radiation Research in Oncology, Dresden, Germany

INTRODUCTION

The combination of MRI and PET for clinical application has recently become feasible as a result of advances in both technologies. The quantitative nature of PET, which provides the absolute activity concentration in a specific voxel, can provide complementary functional information for structural MR imaging and could be combined with simultaneously collected fMRI data. While significant work has been done to address hardware interference, little has been done concerning potential physiologic interference in a combined system. The MR-PET environment is significantly different from the traditional PET environment; in clinical FDG-PET imaging it is common to isolate the patient in a quiet environment for the initial uptake phase. In a multi-modal system, using this time for simultaneous MR imaging could significantly reduce total scan time, however the repetitive acoustic noise of the MR environment can reach as high as 131 dB [1], and has been shown using fMRI to directly stimulate the auditory cortex, requiring the development of specialized paradigms to minimize signal artifacts from acoustic noise [2]. As FDG-PET images metabolism, the acoustic noise can lead to artifacts in the form of focal uptake of FDG. These artifacts can, in turn, significantly impact the metabolic patterns observed in dementia or brain tumor studies. This study sought to examine any effects in the primary auditory cortex in the PET data resulting from MR acoustic noise.

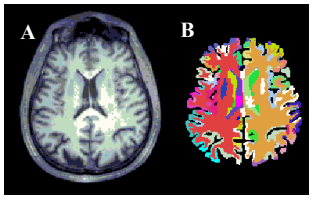

Fig.1: (A) ME-MPRAGE and (B) Freesurfer brain segmentation.

MATERIALS AND METHODS

Integrated MR-PET Scanner: The BrainPET, a MR-compatible brain PET scanner prototype installed at our site, was used for these experiments. This system operates while inserted into the bore of the Siemens 3T TIM Trio MR scanner [3].

Data Acquisition Protocol: Three healthy volunteers were each imaged on two consecutive days either in the presence or absence of MR acoustic noise. To prevent hearing loss, standard earplugs with a noise reduction rating of 29 dB were used, however the acoustic noise of the MR scanner remained clearly audible. Prior to PET data collection, an MR localizer was run to assess subject position in the imaging field of view. PET data acquisition was then started and the volunteer was subsequently intravenously injected with ~5 mCi of FDG. To collect the baseline measurement (i.e. no MR acoustic noise), no MR sequences were run for the next 40 minutes during PET data acquisition. After the first 40 minutes, high resolution anatomical data were acquired using an ME-MPRAGE sequence (1mm^3 isotropic, TR/TI/TE=2530/1200/1.64 ms, flip angle=7^o, TA=4:56 min). Additionally, a dual ultra-short echo sequence (DUTE; 1.67mm^3 isotropic, TR/TE1/TE2 =200/0.07/2.24 ms, flip angle=10^o, TA=3:20 min) was run for attenuation correction purposes if no CT data were available [4]. For measurement with auditory stimulation, MR sequences that are part of our standard brain tumor protocol (i.e. T2-SPACE, FLAIR, BOLD, MEFLASH, T1 mapping, DCE, DTI) were run immediately after injection.

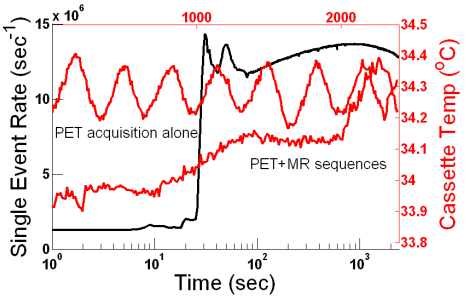

Fig.2: (Black) A typical head curve from a dynamic PET study in the BrainPET. The time of injection can clearly be determined and the singles rate can be used for dead-time correction. (Red) Average temperature of the PET cassettes over data collection show little change over the operation of the camera.

MR-derived cortical segmentation and registration: A high-resolution dataset was acquired using an ME-MPRAGE sequence during each visit (Fig. 1a) and cortical structures of interest (i.e. Heschl's Gyri) were segmented and identified on these images using Freesurfer (Fig 1b) [5]. The affine transformation accounting for differences between the MR and PET space was applied to the segmentation maps and subsequent analysis was performed in the PET coordinate system.

MR-PET Data Analysis: The list-mode PET data acquired during the first 40 minutes after injection were framed into 180 second intervals. Additionally, single frames were generated from the next 15 minutes of data. Corrections were applied to account for variable detector efficiency and deadtime, random coincidences, photon attenuation and scatter, and PET volumes were reconstructed using a 3D-OSEM algorithm. All of the reconstructed images were decay corrected to the time of injection. In order to account for variability with respect to injected dose and subject weight, standard uptake values (SUVs) that were corrected for lean body mass were used. A ROI mask was generated from the Freesurfer segmentation corresponding to the left and right Heschl's Gyri. Average SUVs for all the voxels included in these structures were determined for each of the frames.

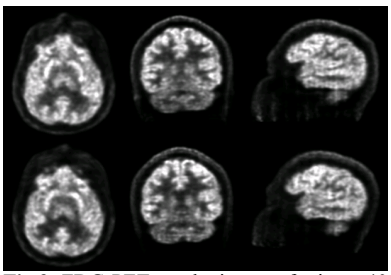

Fig.3: FDG-PET uptake image of minute 40 to 60 post injection; (Top) No MR acoustic stimuli between minutes 0 to 40; (Bot.) MR acoustic stimuli present for minutes 0 to 60.

RESULTS AND DISCUSSIONS

MR interference on PET acquisition: Temperature changes of 0.5^{o}C were observed in the PET cassettes during simultaneous MR-PET acquisition (Fig. 2). However, the head curve (a measurement of the total number of single events detected by the system per second) was free of any significant spikes or deformations when compared to the control case. This suggests that the minimal increase in temperature (likely due to the eddy currents induced in the detector shielding) is adequately compensated for by the temperature control mechanisms of the system and it doesn't affect the PET measurements. Furthermore, it appears that there is no RF interference on the PET detectors from the running sequences.

MR acoustic noise stimulation: The qualitative analysis of the PET volumes obtained at the two visits did not reveal any brain regions with significant changes in FDG uptake. Images from a representative subject are displayed in Fig. 3. The corresponding time activity curves (TACs) for the same subject are show in Fig. 4. The TACs obtained for structures of interest (e.g. Heschl's Gyrus, white matter) matched very closely. The minimal change observed could be explained by other factors such as relative changes in cerebral blood flow, ROI placement, or perhaps patient motion. Similar results were obtained in all three subjects.

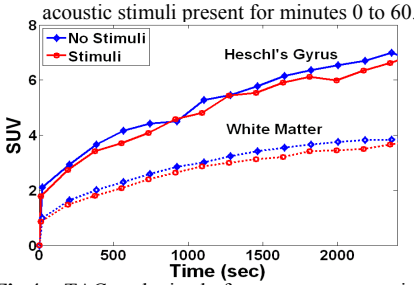

Fig.4: TACs obtained from a representative subject in structures of interest segmented from the simultaneously acquired MR in both the presence and absence of MR acoustic noise.

CONCLUSION: Minimal change was noted between the time activity curves in the stimulus and control cases. As we consider the operation of a simultaneous MR-PET system from a physiologic perceptive, it would appear that MR can be performed during the PET uptake phase without concern of artifacts. As such, it is very likely that traditional fMRI paradigms can be performed on a MR-PET without significant alteration.

REFERENCES: [1] Ravicz, ME et al, J Acoust Soc Am, 2000; 108(4): 1683–1696. [2] Edminster WB et al, Hum. Brain Mapping, 1999; [3] Schlemmer HP et al, Radiol, 2008; 248(3):1028-35; [4] Catana C et al, J Nucl Med, 2010; 51(9): 1431-8 [5] Fischl B et al, Neuron, 2002; 33(3): 341-355.